

I. Introduction

The VINS-Mono[1, 2] is a monocular visual-inertial 6 DOF state estimator proposed by Aerial Robotics Group at HKUST in 2017. It can be performed on MAVs, smartphones and many other intelligent platforms. It is a state-of-the-art visual-inertial odometry algorithms which has gained extensive attention worldwide. SLAM is considered as a key technology for autonomous mobile robots due to its ability to navigation in unknown environments independently. The whole framework of the VINS-Mono is shown as Figure 1. As far as I am concerned, the most excellent works of it are as follow:

1. A robust initialization procedure which can produce a comparatively accurate estimation of the visual scale, the gravity, the velocity and gyroscope bias.
2. Sliding window based local optimization.
3. Online relocalization and 4 DOF global pose graph optimization.

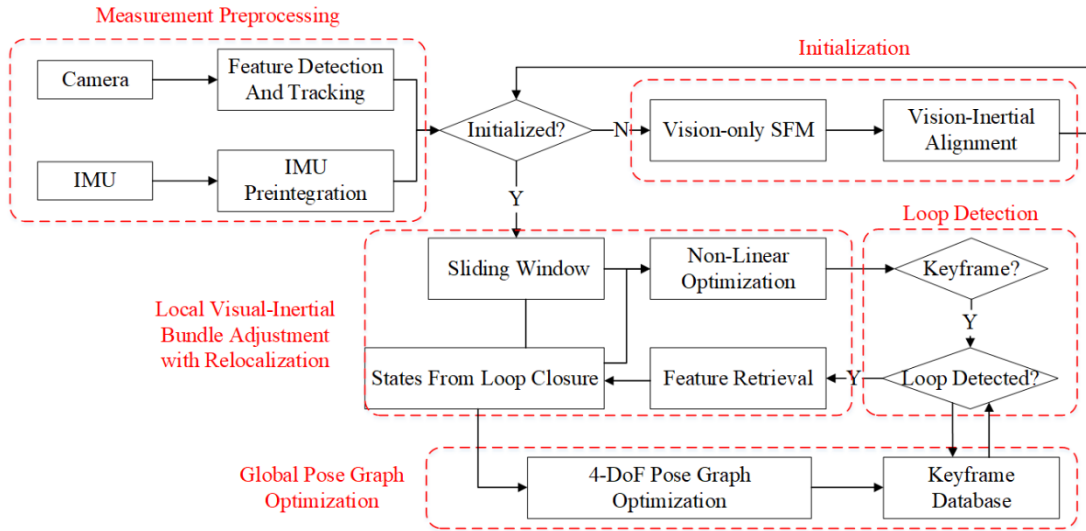


Figure 1 Framework overview of the VINS-Mono (Shaojie Shen, 2017)

The manuscript is organized as follows: The process of IMU preintegration is described in Section II. Section III presents the visual/inertial co-initialization procedure. The tightly-coupled nonlinear optimization is then introduced in Section IV. Section V describes the marginalization procedure. The equations of global optimization with GPS in VINS-Fusion, an extension of VIN-Mono, are also provided in Section VI. Please see the Appendix for details of some equation derivation.

Nomenclature

- a) Matrices are denoted in upper case bold letters.
- b) Vectors are denoted in lower case bold italic letters.
- c) Scalar is denoted in lower case italic letters.
- d) The coordinate frames involved in the vector transformation are denoted as superscript and subscript. For vectors, the superscript denotes the projected coordinate system.

- e) $\hat{*}$, estimated or computed values.
- f) $\tilde{*}$, observed or measured values.
- g) a_x , element of vector \mathbf{a} on x axis.

II. IMU Preintegration

2.1 IMU Preintegration in Continuous Time

The IMU preintegration is proposed in [3, 4]. In most practical applications, the IMU data rate is faster than that of the camera, which means that there are several IMU measurements between every two consecutive frames, as shown in Figure 2. First of all, we have to know that an IMU consists of a gyroscope and an accelerometer to measure the angular rate and acceleration of the IMU w.r.t. the inertial frame, respectively. For accelerometer, its measurement can be written as

$$\mathbf{f}^b = \mathbf{a}^b - \mathbf{g}^b \quad (1)$$

where \mathbf{f} is the special force, \mathbf{a} is the true acceleration of the IMU, \mathbf{g} is the local gravity. It means that the output of the accelerometer is not the true acceleration of the IMU, but the acceleration minus gravity. If the IMU frame is defined as right-front-up, its measurement will be

$\mathbf{f}_0^b = -\mathbf{g}^b$ when the IMU keep static and level.

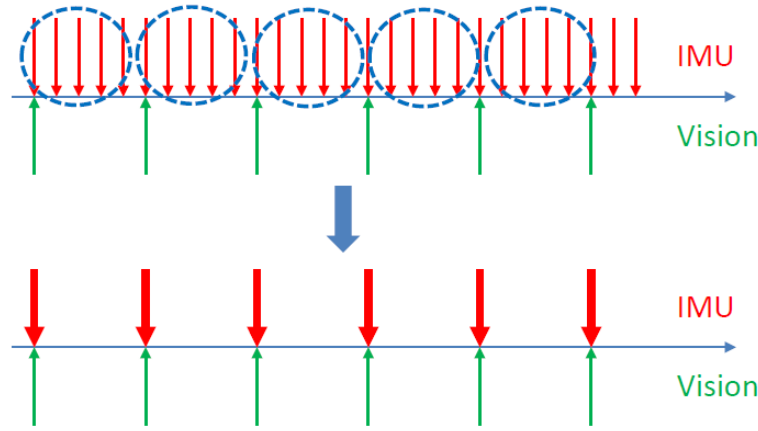


Figure 2 Diagrammatic drawing of IMU preintegration

Given two time instants that correspond to images frame b_k and b_{k+1} , the state variables are constrained by inertial measurements during time interval $[k, k+1]$:

$$\begin{aligned}
\mathbf{p}_{b_{k+1}}^w &= \mathbf{p}_{b_k}^w + \mathbf{v}_{b_k}^w \Delta t_k + \iint_{t \in [k, k+1]} (\mathbf{R}_t^w (\hat{\mathbf{a}}_t - \mathbf{b}_{at}) - \mathbf{g}^w) dt^2 \\
\mathbf{v}_{b_{k+1}}^w &= \mathbf{v}_{b_k}^w + \int_{t \in [k, k+1]} (\mathbf{R}_t^w (\hat{\mathbf{a}}_t - \mathbf{b}_{at}) - \mathbf{g}^w) dt \\
\mathbf{q}_{b_{k+1}}^w &= \mathbf{q}_{b_k}^w \otimes \int_{t \in [k, k+1]} \frac{1}{2} \mathbf{\Omega}(\hat{\boldsymbol{\omega}}_t - \mathbf{b}_{gt}) \mathbf{q}_t^{b_k} dt
\end{aligned} \tag{2}$$

CAUTION: The \mathbf{g}^w here does not mean the gravity in world coordinates but the projection of \mathbf{f}_0^b in world coordinates.

Where

$$\mathbf{\Omega}_R(\boldsymbol{\omega}) = [\boldsymbol{\omega}]_R = \begin{bmatrix} 0 & -\boldsymbol{\omega}^T \\ \boldsymbol{\omega} & (\boldsymbol{\omega}) \times \end{bmatrix}, (\boldsymbol{\omega}) \times = \begin{bmatrix} 0 & -\omega_z & \omega_y \\ \omega_z & 0 & -\omega_x \\ -\omega_y & \omega_x & 0 \end{bmatrix} \tag{3}$$

For the last equation in (2), we have the following according to [5]

$$\begin{aligned}
\dot{\mathbf{q}} &\triangleq \lim_{\delta t \rightarrow 0} \frac{\mathbf{q}(t + \delta t) - \mathbf{q}(t)}{\delta t} \\
&= \lim_{\delta t \rightarrow 0} \frac{\mathbf{q}(t) \otimes \delta \mathbf{q} - \mathbf{q}(t)}{\delta t} \\
&= \lim_{\delta t \rightarrow 0} \frac{\mathbf{q}(t) \otimes \left(\begin{bmatrix} 1 \\ \delta \boldsymbol{\theta} / 2 \end{bmatrix} - \begin{bmatrix} 1 \\ 0 \end{bmatrix} \right)}{\delta t} \\
&= \frac{1}{2} \mathbf{q} \otimes \boldsymbol{\omega}_t = \frac{1}{2} \mathbf{\Omega}_R(\boldsymbol{\omega}_t) \mathbf{q}
\end{aligned} \tag{4}$$

In this report, we define that $\mathbf{q} = [q_w \quad \mathbf{q}_v]^T = [q_w \quad q_x \quad q_y \quad q_z]^T$.

Change the reference frame for IMU propagation to local frame b_k , we can only integrate the parts which are related to linear acceleration $\hat{\mathbf{a}}$ and angular velocity $\hat{\boldsymbol{\omega}}$ as follows:

$$\begin{aligned}
\mathbf{R}_w^{b_k} \mathbf{p}_{b_{k+1}}^w &= \mathbf{R}_w^{b_k} (\mathbf{p}_{b_k}^w + \mathbf{v}_{b_k}^w \Delta t_k - \frac{1}{2} \mathbf{g}^w \Delta t_k^2) + \boldsymbol{\alpha}_{b_{k+1}}^{b_k} \\
\mathbf{R}_w^{b_k} \mathbf{v}_{b_{k+1}}^w &= \mathbf{R}_w^{b_k} (\mathbf{v}_{b_k}^w - \mathbf{g}^w \Delta t_k) + \boldsymbol{\beta}_{b_{k+1}}^{b_k} \\
\mathbf{q}_w^{b_k} \mathbf{q}_{b_{k+1}}^w &= \boldsymbol{\gamma}_{b_{k+1}}^{b_k}
\end{aligned} \tag{5}$$

where

$$\begin{aligned}
\alpha_{b_{k+1}}^{b_k} &= \iint_{t \in [k, k+1]} \mathbf{R}_t^{b_k} (\hat{\mathbf{a}}_t - \mathbf{b}_{at}) dt^2 \\
\beta_{b_{k+1}}^{b_k} &= \int_{t \in [k, k+1]} \mathbf{R}_t^{b_k} (\hat{\mathbf{a}}_t - \mathbf{b}_{at}) dt \\
\gamma_{b_{k+1}}^{b_k} &= \int_{t \in [k, k+1]} \frac{1}{2} \mathbf{\Omega}(\hat{\boldsymbol{\omega}}_t - \mathbf{b}_{gt}) \mathbf{q}_t^{b_k} dt
\end{aligned} \tag{6}$$

2.2 IMU Preintegration in Discrete Time

As for the discrete-time implementation, we can apply Mid-point method as follow

$$\begin{aligned}
\gamma_{i+1}^{b_k} &= \gamma_i^{b_k} \otimes \gamma_{i,i+1}^{b_k} = \gamma_i^{b_k} \otimes \left[\begin{array}{c} 1 \\ 1/2(\boldsymbol{\omega}_i + \boldsymbol{\omega}_{i+1} - 2\mathbf{b}_{gi})\delta t \end{array} \right] \\
\beta_{i+1}^{b_k} &= \int_{t \in [k, i]} (\dots) dt + \int_{t \in [i, i+1]} (\dots) dt \\
&= \beta_i^{b_k} + \frac{1}{2} \left[\mathbf{R}(\gamma_i^{b_k})(\hat{\mathbf{a}}_i - \mathbf{b}_{ai}) + \mathbf{R}(\gamma_{i+1}^{b_k})(\hat{\mathbf{a}}_{i+1} - \mathbf{b}_{ai}) \right] \delta t \\
\alpha_{i+1}^{b_k} &= \alpha_i^{b_k} + \frac{1}{2} (\beta_i^{b_k} + \beta_{i+1}^{b_k}) \delta t \\
&= \alpha_i^{b_k} + \beta_i^{b_k} \delta t + \frac{1}{4} \left[\mathbf{R}(\gamma_i^{b_k})(\hat{\mathbf{a}}_i - \mathbf{b}_{ai}) + \mathbf{R}(\gamma_{i+1}^{b_k})(\hat{\mathbf{a}}_{i+1} - \mathbf{b}_{ai}) \right] \delta t^2
\end{aligned} \tag{7}$$

CAUTION: Strictly speaking, the preintegration values $\alpha_{b_{k+1}}^{b_k}$ and $\beta_{b_{k+1}}^{b_k}$ do not have any physical meaning except the attitude, since the gravity is ignored. However, we can imagine a zero gravity space in which the measurement of accelerometer will be the real acceleration, then (6) (7) will become easy to understand.

2.3 Error-state Kinematics in Continuous Time

Inspired by [5], we can write the error-state equations of the kinematics of an inertial system. We introduce the error perturbation analysis,

$$\hat{\mathbf{x}} = \mathbf{x} + \delta \mathbf{x} \tag{8}$$

where \mathbf{x} is the ideal(or nominal [5]) value of the sensors measurements or the body state without any error, $\hat{\mathbf{x}}$ is the calculated(or observed, or true [5])value of measurements and body state which contain errors $\delta \mathbf{x}$.

For the ideal-state kinematics, we have

$$\begin{aligned}
\dot{\alpha} &= \beta \\
\dot{\beta} &= \mathbf{R}(\mathbf{a}_m - \mathbf{b}_a) \\
\dot{\gamma} &= \frac{1}{2} \gamma \otimes (\omega_m - \mathbf{b}_\omega) \\
\dot{\mathbf{b}}_a &= 0 \\
\dot{\mathbf{b}}_\omega &= 0
\end{aligned} \tag{9}$$

For the calculated-state, we have

$$\begin{aligned}
\dot{\hat{\alpha}} &= \hat{\beta} \\
\dot{\hat{\beta}} &= \hat{\mathbf{R}}(\mathbf{a}_m - \mathbf{n}_a - \hat{\mathbf{b}}_a) \\
\dot{\hat{\gamma}} &= \frac{1}{2} \hat{\gamma} \otimes (\omega_m - \mathbf{n}_\omega - \hat{\mathbf{b}}_g) \\
\dot{\hat{\mathbf{b}}}_a &= \mathbf{n}_{b_a} \\
\dot{\hat{\mathbf{b}}}_\omega &= \mathbf{n}_{b_\omega}
\end{aligned} \tag{10}$$

Assume the acceleration bias and gyroscope bias are random walk, whose derivatives are Gaussian white noise, i.e., $n_{b_a} \sim N(0, \sigma_{b_a}^2)$, $n_{b_\omega} \sim N(0, \sigma_{b_\omega}^2)$. The noise in acceleration \mathbf{a}_m and gyroscope measurements ω_m are treated as the same.

Then, we have the error-state kinematics,

$$\begin{aligned}
\dot{\delta\alpha} &= \delta\beta \\
\dot{\delta\beta} &= -\mathbf{R}(\mathbf{a}_m - \mathbf{b}_a) \times \delta\theta - \mathbf{R}n_a - \mathbf{R}\delta\mathbf{b}_a \\
\dot{\delta\theta} &= -(\omega_m - \mathbf{b}_g) \times \delta\theta - \delta\mathbf{b}_g - \mathbf{n}_\omega \\
\dot{\delta\mathbf{b}}_a &= \mathbf{n}_{b_a} \\
\dot{\delta\mathbf{b}}_g &= \mathbf{n}_{b_g}
\end{aligned} \tag{11}$$

Proofs of equations of velocity and attitude errors are developed as follow, the second-order small terms are so trivial that we can ignore it,

$$\begin{aligned}
\dot{\beta} + \delta\dot{\beta} &= \dot{\hat{\beta}} = \hat{\mathbf{R}}(\mathbf{a}_m - \mathbf{n}_a - \hat{\mathbf{b}}_a) \\
\mathbf{R}(\mathbf{a}_m - \mathbf{b}_a) + \delta\dot{\beta} &= \dot{\hat{\beta}} = \mathbf{R}[\mathbf{I} + (\delta\theta) \times](\mathbf{a}_m - \mathbf{n}_a - \mathbf{b}_a - \delta\mathbf{b}_a) \\
\dot{\delta\beta} &= -\mathbf{R}(\mathbf{a}_m - \mathbf{b}_a) \times \delta\theta - \mathbf{R}n_a - \mathbf{R}\delta\mathbf{b}_a
\end{aligned} \tag{12}$$

$$\begin{aligned}
\gamma \otimes \dot{\delta\gamma} &= \dot{\hat{\gamma}} = \frac{1}{2} \hat{\gamma} \otimes (\omega_m - n_\omega - \hat{b}_g) \\
\dot{\gamma} \otimes \delta\gamma + \gamma \otimes \dot{\delta\gamma} &= \dot{\hat{\gamma}} = \frac{1}{2} \gamma \otimes \delta\gamma \otimes (\omega_m - n_\omega - b_g - \delta b_\omega) \\
\frac{1}{2} \gamma \otimes (\omega_m - b_g) \otimes \delta\gamma + \gamma \otimes \dot{\delta\gamma} &= \frac{1}{2} \gamma \otimes \delta\gamma \otimes (\omega_m - n_\omega - b_g - \delta b_g) \\
\text{let } (\hat{\omega} &= \omega_m - n_\omega - b_g - \delta b_g, \omega = \omega_m - b_g) \\
2 \dot{\delta\gamma} &= \delta\gamma \otimes \hat{\omega} - \omega \otimes \delta\gamma \\
&= \Omega_R(\hat{\omega}) \delta\gamma - \Omega_L(\omega) \delta\gamma \\
&= \begin{bmatrix} 0 & (\omega - \hat{\omega})^T \\ \hat{\omega} - \omega & -(\omega + \hat{\omega}) \times \end{bmatrix} \delta\gamma \\
\begin{bmatrix} 0 \\ \dot{\delta\theta} \end{bmatrix} &= \begin{bmatrix} 0 & (\delta b_g + n_\omega)^T \\ -\delta b_g - n_\omega & -(2\omega_m - n_\omega - 2b_g - \delta b_g) \times \end{bmatrix} \begin{bmatrix} 1 \\ \frac{1}{2} \delta\theta \end{bmatrix} \\
\dot{\delta\theta} &= -(\omega_m - b_g) \times \delta\theta - \delta b_g - n_\omega
\end{aligned} \tag{13}$$

Then, we have

$$\begin{bmatrix} \delta\dot{\alpha}_t^{b_k} \\ \delta\dot{\beta}_t^{b_k} \\ \delta\dot{\theta}_t^{b_k} \\ \delta\dot{b}_{a_t} \\ \delta\dot{b}_{g_t} \end{bmatrix} = \begin{bmatrix} \mathbf{I} & & & & \\ & -\mathbf{R}_t^{b_k} (a_m - b_a) \times & -\mathbf{R}_t^{b_k} & & \\ & -(\omega_m - b_g) \times & & -\mathbf{I} & \\ & & & & \mathbf{I} \\ & & & & & \mathbf{I} \end{bmatrix} \begin{bmatrix} \delta\alpha_t^{b_k} \\ \delta\beta_t^{b_k} \\ \delta\theta_t^{b_k} \\ \delta b_{a_t} \\ \delta b_{\omega_t} \end{bmatrix} + \begin{bmatrix} & -\mathbf{R}_t^{b_k} & & & \\ & & -\mathbf{I} & & \\ & & & \mathbf{I} & \\ & & & & \mathbf{I} \end{bmatrix} \begin{bmatrix} n_a \\ n_\omega \\ n_{b_a} \\ n_{b_\omega} \end{bmatrix} \tag{14}$$

$$\delta\dot{\mathbf{x}}_t = \mathbf{F}_t \delta\mathbf{x}_t + \mathbf{G}_t \mathbf{n}_t \tag{15}$$

As we all know,

$$\dot{\mathbf{x}} = \lim_{\delta t \rightarrow \infty} \frac{\mathbf{x}(t + \delta t) - \mathbf{x}(t)}{\delta t} \tag{16}$$

Within a small time interval, we have

$$\delta\mathbf{x}_{t+\delta t} = (\mathbf{I} + \mathbf{F}_t \delta t) \delta\mathbf{x}_t + \mathbf{G}_t \mathbf{n}_t \delta t \tag{17}$$

$\mathbf{P}_{b_{k+1}}^{b_k}$ can be computed recursively by the first-order discrete-time covariance updating with the initial covariance $\mathbf{P}_{b_k}^{b_k} = 0$:

$$\mathbf{P}_{t+\delta t}^{b_k} = (\mathbf{I} + \mathbf{F}_t \delta t) \mathbf{P}_t^{b_k} (\mathbf{I} + \mathbf{F}_t \delta t)^T + (\mathbf{G}_t \delta t) \mathbf{Q} (\mathbf{G}_t \delta t)^T \tag{18}$$

Where δt is the time between two IMU measurements, and \mathbf{Q} is the diagonal covariance matrix of noise $\text{diag}(\sigma_a^2, \sigma_\omega^2, \sigma_{b_a}^2, \sigma_{b_\omega}^2)$.

Meanwhile, the first-order Jacobian matrix $\mathbf{J}_{b_{k+1}}^{b_k}$ of $\delta \mathbf{x}_{b_{k+1}}^{b_k}$ w.r.t $\delta \mathbf{x}_{b_k}^{b_k}$ can be compute recursively with the initial Jacobian $\mathbf{J}_{b_k}^{b_k} = \mathbf{I}$,

$$\mathbf{J}_{t+\delta t} = (\mathbf{I} + \mathbf{F}_t \delta t) \mathbf{J}_t, t \in [k, k+1] \quad (19)$$

Consider the variables associated with the preintegration, the first order approximation of $(\boldsymbol{\alpha}_{b_{k+1}}^{b_k}, \boldsymbol{\beta}_{b_{k+1}}^{b_k}, \boldsymbol{\gamma}_{b_{k+1}}^{b_k})$ can be wrote as

$$\begin{aligned} \boldsymbol{\alpha}_{b_{k+1}}^{b_k} &\approx \hat{\boldsymbol{\alpha}}_{b_{k+1}}^{b_k} + \mathbf{J}_{b_a}^\alpha \delta \mathbf{b}_{ak} + \mathbf{J}_{b_g}^\alpha \delta \mathbf{b}_{gk} \\ \boldsymbol{\beta}_{b_{k+1}}^{b_k} &\approx \hat{\boldsymbol{\beta}}_{b_{k+1}}^{b_k} + \mathbf{J}_{b_a}^\beta \delta \mathbf{b}_{ak} + \mathbf{J}_{b_g}^\beta \delta \mathbf{b}_{gk} \\ \boldsymbol{\gamma}_{b_{k+1}}^{b_k} &= \hat{\boldsymbol{\gamma}}_{b_{k+1}}^{b_k} \otimes \begin{bmatrix} 1 \\ \frac{1}{2} \mathbf{J}_{b_g}^\gamma \delta \mathbf{b}_{gk} \end{bmatrix} \end{aligned} \quad (20)$$

where $\mathbf{J}_{b_a}^\alpha$ is the sub-block matrix in $\mathbf{J}_{b_{k+1}}$ whose location is corresponding to $\frac{\delta \mathbf{x}_{b_{k+1}}^{b_k}}{\delta \mathbf{b}_a}$, the others are of the same meaning.

2.4 Error-state Kinematics in Discrete Time

We assume the bias of sensors between two IMU measurements are constant. According to (17) and using the Mid-point integration for discrete time implementation, we have

$$\begin{cases}
\dot{\delta\theta}_t^{b_k} = -\left(\frac{\omega_t + \omega_{t+1}}{2} - \mathbf{b}_{\omega_t}\right) \times \delta\theta_t^{b_k} - \delta\mathbf{b}_{g_t} - \frac{\mathbf{n}_{\omega_t} + \mathbf{n}_{\omega_{t+1}}}{2} \\
\delta\theta_{t+1}^{b_k} = \left[\mathbf{I} - \delta t \left(\frac{\omega_t + \omega_{t+1}}{2} - \mathbf{b}_{g_t}\right) \times\right] \delta\theta_t^{b_k} - \delta\mathbf{b}_{g_t} \delta t - \frac{\mathbf{n}_{\omega_t} + \mathbf{n}_{\omega_{t+1}}}{2} \delta t \\
\dot{\delta\beta}_t^{b_k} = -\mathbf{R}_t^{b_k} (\mathbf{a}_t - \mathbf{b}_{a_t}) \times \delta\theta_t^{b_k} - \mathbf{R}_t^{b_k} \delta\mathbf{b}_{a_t} - \mathbf{R}_t^{b_k} \mathbf{n}_{a_t} \\
= -\frac{1}{2} \mathbf{R}_t^{b_k} (\mathbf{a}_t - \mathbf{b}_{a_t}) \times \delta\theta_t^{b_k} - \frac{1}{2} \mathbf{R}_{t+1}^{b_k} (\mathbf{a}_{t+1} - \mathbf{b}_{a_t}) \times \delta\theta_{t+1}^{b_k} - \frac{1}{2} (\mathbf{R}_t^{b_k} + \mathbf{R}_{t+1}^{b_k}) \delta\mathbf{b}_{a_t} \\
- \frac{1}{2} (\mathbf{R}_t^{b_k} + \mathbf{R}_{t+1}^{b_k}) \mathbf{n}_{a_t} \\
\delta\beta_{t+1}^{b_k} = \left\{ -\frac{\delta t}{2} \mathbf{R}_t^{b_k} (\mathbf{a}_t - \mathbf{b}_{a_t}) \times -\frac{\delta t^2}{2} \mathbf{R}_{t+1}^{b_k} (\mathbf{a}_{t+1} - \mathbf{b}_{a_t}) \times \left[\mathbf{I} - \delta t \left(\frac{\omega_t + \omega_{t+1}}{2} - \mathbf{b}_{g_t}\right) \times\right] \right\} \delta\theta_t^{b_k} \\
+ \frac{\delta t^2}{2} \mathbf{R}_{t+1}^{b_k} (\mathbf{a}_{t+1} - \mathbf{b}_{a_t}) \times \delta\mathbf{b}_{g_t} - \frac{1}{2} (\mathbf{R}_t^{b_k} + \mathbf{R}_{t+1}^{b_k}) \delta\mathbf{b}_{a_t} + \frac{\delta t^2}{4} \mathbf{R}_{t+1}^{b_k} (\mathbf{a}_{t+1} - \mathbf{b}_{a_t}) \times \mathbf{n}_{\omega_t} \\
+ \frac{\delta t^2}{4} \mathbf{R}_{t+1}^{b_k} (\mathbf{a}_{t+1} - \mathbf{b}_{a_t}) \times \mathbf{n}_{\omega_{t+1}} - \frac{\delta t}{2} \mathbf{R}_t^{b_k} \mathbf{n}_{a_t} - \frac{\delta t}{2} \mathbf{R}_{t+1}^{b_k} \mathbf{n}_{a_{t+1}} + \delta\beta_t^{b_k} \\
\dot{\delta\alpha}_t^{b_k} = \frac{1}{2} (\delta\beta_t^{b_k} + \delta\beta_{t+1}^{b_k}) \\
\delta\alpha_{t+1}^{b_k} = \delta\alpha_t^{b_k} + \frac{1}{2} (\delta\beta_t^{b_k} + \delta\beta_{t+1}^{b_k}) \delta t
\end{cases} \quad (21)$$

We can write it in matrix form as follows (This is mostly according with the code. See “midPointIntegration” in “integration_base.h” in [2].),

$$\begin{bmatrix} \delta\alpha_{k+1} \\ \delta\theta_{k+1} \\ \delta\beta_{k+1} \\ \delta\mathbf{b}_{ak+1} \\ \delta\mathbf{b}_{gk+1} \end{bmatrix} = \begin{bmatrix} \mathbf{I} & \mathbf{F}_{01} & \delta t & \mathbf{F}_{03} & \mathbf{F}_{04} \\ \mathbf{0} & \mathbf{F}_{11} & \mathbf{0} & \mathbf{0} & -\delta t \\ \mathbf{0} & \mathbf{F}_{21} & \mathbf{I} & \mathbf{F}_{23} & \mathbf{F}_{24} \\ \mathbf{0} & \mathbf{0} & \mathbf{0} & \mathbf{I} & \mathbf{0} \\ \mathbf{0} & \mathbf{0} & \mathbf{0} & \mathbf{0} & \mathbf{I} \end{bmatrix} \begin{bmatrix} \delta\alpha_k \\ \delta\theta_k \\ \delta\beta_k \\ \delta\mathbf{b}_{ak} \\ \delta\mathbf{b}_{gk} \end{bmatrix} \\
+ \begin{bmatrix} \mathbf{G}_{00} & \mathbf{G}_{01} & \mathbf{G}_{02} & \mathbf{G}_{03} & \mathbf{0} & \mathbf{0} \\ \mathbf{0} & -\delta t / 2 & \mathbf{0} & -\delta t / 2 & \mathbf{0} & \mathbf{0} \\ \frac{-\mathbf{R}_k \delta t}{2} & \mathbf{G}_{21} & \frac{-\mathbf{R}_{k+1} \delta t}{2} & \mathbf{G}_{23} & \mathbf{0} & \mathbf{0} \\ \mathbf{0} & \mathbf{0} & \mathbf{0} & \mathbf{0} & \delta t & \mathbf{0} \\ \mathbf{0} & \mathbf{0} & \mathbf{0} & \mathbf{0} & \mathbf{0} & \delta t \end{bmatrix} \begin{bmatrix} \mathbf{n}_{a_k} \\ \mathbf{n}_{g_k} \\ \mathbf{n}_{a_{k+1}} \\ \mathbf{n}_{g_{k+1}} \\ \mathbf{n}_{b_a} \\ \mathbf{n}_{b_g} \end{bmatrix} \quad (22)$$

where,

$$\begin{aligned}\mathbf{F}_{01} &= -\frac{\delta t^2}{4} \mathbf{R}_k (\hat{\mathbf{a}}_k - \mathbf{b}_{ak}) \times -\frac{\delta t^2}{4} \mathbf{R}_{k+1} (\hat{\mathbf{a}}_{k+1} - \mathbf{b}_{ak}) \times \left[\mathbf{I} - \left(\frac{\hat{\boldsymbol{\omega}}_k + \hat{\boldsymbol{\omega}}_{k+1}}{2} - \mathbf{b}_{\omega k} \right) \times \delta t \right] \\ \mathbf{F}_{03} &= -\frac{\delta t^2}{4} (\mathbf{R}_k + \mathbf{R}_{k+1})\end{aligned}\quad (23)$$

$$\begin{aligned}\mathbf{F}_{04} &= \frac{\delta t^3}{4} \mathbf{R}_{k+1} (\hat{\mathbf{a}}_{k+1} - \mathbf{b}_{ak}) \times \\ \mathbf{F}_{11} &= \mathbf{I} - \left(\frac{\hat{\boldsymbol{\omega}}_k + \hat{\boldsymbol{\omega}}_{k+1}}{2} - \mathbf{b}_{gk} \right) \times \delta t\end{aligned}\quad (24)$$

$$\begin{aligned}\mathbf{F}_{21} &= -\frac{\delta t}{2} \mathbf{R}_k (\hat{\mathbf{a}}_k - \mathbf{b}_{ak}) \times -\frac{\delta t}{2} \mathbf{R}_{k+1} (\hat{\mathbf{a}}_{k+1} - \mathbf{b}_{ak}) \times \left[\mathbf{I} - \delta t \left(\frac{\hat{\boldsymbol{\omega}}_k + \hat{\boldsymbol{\omega}}_{k+1}}{2} - \mathbf{b}_{gk} \right) \times \right] \\ \mathbf{F}_{23} &= -\frac{\delta t}{2} (\mathbf{R}_k + \mathbf{R}_{k+1}) \\ \mathbf{F}_{24} &= \frac{\delta t^2}{2} \mathbf{R}_{k+1} (\hat{\mathbf{a}}_{k+1} - \mathbf{b}_{ak}) \times\end{aligned}\quad (25)$$

$$\begin{aligned}\mathbf{G}_{00} &= -\frac{\delta t^2}{4} \mathbf{R}_k \\ \mathbf{G}_{01} = \mathbf{G}_{03} &= \frac{\delta t^3}{8} \mathbf{R}_{k+1} (\hat{\mathbf{a}}_{k+1} - \mathbf{b}_{ak}) \times\end{aligned}\quad (26)$$

$$\begin{aligned}\mathbf{G}_{02} &= -\frac{\delta t^2}{4} \mathbf{R}_{k+1} \\ \mathbf{G}_{21} = \mathbf{G}_{23} &= \frac{\delta t^2}{4} \mathbf{R}_{k+1} (\hat{\mathbf{a}}_{k+1} - \mathbf{b}_{ak}) \times\end{aligned}\quad (27)$$

III. Initialization

The initialization procedure can be divided into four major steps as shown in Figure 3.

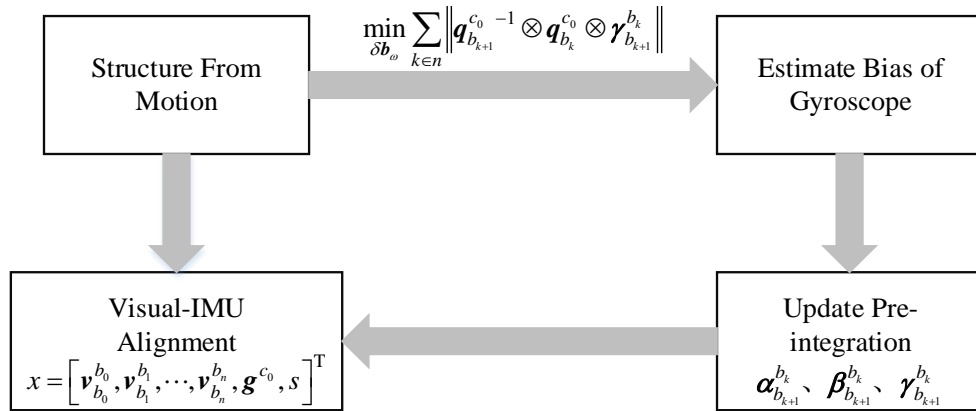


Figure 3 Initialization procedure

It starts with a vision-only structure from motion (SFM) in the sliding window. Firstly, we recover the relative pose (up-to-scale) between two image frames by Five-point method when we can find a previous frame which has more than thirty tracked features and the average parallax is more than twenty pixels between it and the latest frame. We set this frame (not always the first frame in the code) as the reference frame (c_0) for the moment. Then we triangulate all the features between the two frames. We perform EPnP[6] to estimate poses of other frames in the whole window based on the 3D features. At last, a bundle adjustment is performed to minimize the total reprojection error to optimize all poses in the window.

We can transform the poses from camera center to IMU center according to the extrinsic parameters $\begin{pmatrix} p_c^b & q_c^b \end{pmatrix}$

$$\begin{aligned} q_{b_k}^{c_0} &= q_{c_k}^{c_0} \otimes (q_c^b)^{-1} \\ s\bar{p}_{b_k}^{c_0} &= s\bar{p}_{c_k}^{c_0} - \mathbf{R}_{b_k}^{c_0} p_c^b \end{aligned} \quad (28)$$

where \bar{p} denotes the vector p up to the scale s .

Change the reference frame from the world frame to the c_0 frame in the SFM, we can rewrite the IMU preintegration in (5) as follow:

$$\begin{aligned} \hat{\alpha}_{b_{k+1}}^{b_k} &= \mathbf{R}_{c_0}^{b_k} \left(s \left(\bar{p}_{b_{k+1}}^{c_0} - \bar{p}_{b_k}^{c_0} \right) + \frac{1}{2} \mathbf{g}^{c_0} \delta t^2 - \mathbf{R}_{b_k}^{c_0} \mathbf{v}_{b_k}^{b_k} \delta t \right) \\ \hat{\beta}_{b_{k+1}}^{b_k} &= \mathbf{R}_{c_0}^{b_k} \left(\mathbf{R}_{b_{k+1}}^{c_0} \mathbf{v}_{b_{k+1}}^{b_{k+1}} + \mathbf{g}^{c_0} \delta t - \mathbf{R}_{b_k}^{c_0} \mathbf{v}_{b_k}^{b_k} \right) \end{aligned} \quad (29)$$

From (28) and (29) we can get a system of linear equations, which can be solved easily by matrix decomposition.

$$\begin{aligned} \hat{\alpha}_{b_{k+1}}^{b_k} &= \mathbf{R}_{c_0}^{b_k} \left(s \left(\bar{p}_{b_{k+1}}^{c_0} - \bar{p}_{b_k}^{c_0} \right) + \frac{1}{2} \mathbf{g}^{c_0} \delta t^2 - \mathbf{R}_{b_k}^{c_0} \mathbf{v}_{b_k}^{b_k} \delta t \right) \\ &= \mathbf{R}_{c_0}^{b_k} \left(s\bar{p}_{c_{k+1}}^{c_0} - \mathbf{R}_{b_{k+1}}^{c_0} p_c^b - (s\bar{p}_{c_k}^{c_0} - \mathbf{R}_{b_k}^{c_0} p_c^b) + \frac{1}{2} \mathbf{g}^{c_0} \delta t^2 - \mathbf{R}_{b_k}^{c_0} \mathbf{v}_{b_k}^{b_k} \delta t \right) \\ &= \mathbf{R}_{c_0}^{b_k} \left(\bar{p}_{c_{k+1}}^{c_0} - \bar{p}_{c_k}^{c_0} \right) s + \frac{1}{2} \mathbf{R}_{c_0}^{b_k} \delta t^2 \mathbf{g}^{c_0} - \mathbf{v}_{b_k}^{b_k} \delta t + p_c^b - \mathbf{R}_{c_0}^{b_k} \mathbf{R}_{b_{k+1}}^{c_0} p_c^b \end{aligned} \quad (30)$$

$$\begin{aligned}
& \begin{bmatrix} \hat{\alpha}_{b_{k+1}}^{b_k} - p_c^b + \mathbf{R}_{c_0}^{b_k} \mathbf{R}_{b_{k+1}}^{c_0} p_c^b \\ \hat{p}_{b_{k+1}}^{b_k} \end{bmatrix} = \\
& \begin{bmatrix} -\delta t \mathbf{I} & 0 & \frac{1}{2} \mathbf{R}_{c_0}^{b_k} \delta t^2 & \mathbf{R}_{c_0}^{b_k} (\bar{p}_{c_{k+1}}^{c_0} - \bar{p}_{c_k}^{c_0}) \\ -\mathbf{I} & \mathbf{R}_{c_0}^{b_k} \mathbf{R}_{b_{k+1}}^{c_0} & \delta t \mathbf{R}_{c_0}^{b_k} & 0 \end{bmatrix} \begin{bmatrix} \mathbf{v}_{b_k}^{b_k} \\ \mathbf{v}_{b_{k+1}}^{b_{k+1}} \\ \mathbf{g}^{c_0} \\ s \end{bmatrix} \quad (31)
\end{aligned}$$

The state we estimate in this step is

$$\chi = [\mathbf{v}_{b_0}^{b_0}, \mathbf{v}_{b_1}^{b_1}, \dots, \mathbf{v}_{b_n}^{b_n}, \mathbf{g}^{c_0}, s] \quad (32)$$

Moreover, the estimated gravity vector can be refined by the known magnitude. A vector in a three dimensional space is constraint by its magnitude and projection on three axes. If we know any three values of them, the other one can be uniquely determined. Since the magnitude of gravity is known, the degrees of freedom of gravity is two. We can parameterize the gravity with two variables on its tangent space as follow

$$\mathbf{g}^{c_0} = \|\mathbf{g}\| \frac{\mathbf{g}^{c_0}}{\|\mathbf{g}^{c_0}\|} + [\mathbf{b}_1 \quad \mathbf{b}_2] \begin{bmatrix} w_1 \\ w_2 \end{bmatrix} \quad (33)$$

where \mathbf{g}^{c_0} , \mathbf{b}_1 , \mathbf{b}_2 are orthogonal, \mathbf{b}_1 , \mathbf{b}_2 is generated by vector cross product. We substitute \mathbf{g}^{c_0} in (31) by (33), and solve w_1 and w_2 recursively until converge (when w_1 and w_2 are close to zero).

After refining gravity, we can recover the transformation from the c_0 frame to the world frame by rotating the gravity vector. We set the origin of the world frame at that of the c_0 frame. However, the heading angle can be any value because the number of unknown terms in the rotation matrix is nine (which is more than the knowns). So we can rotate the world frame to ensure the heading angle of the first frame is zero.

Now, the initialization process is completed. We have recovered the scale of visual odometry by aligning the IMU measurements with visual-based SFM. We have established the world frame whose z axis is parallel with the gravity vector. And we have estimated the real-scaled velocity in the world frame.

IV. Tightly-coupled Nonlinear Optimization

4.1 Cost Function

In the back-end optimization procedure, the inverse depth of features (Why inverse depth? Because it has better numerical stability which is convenient to solve [7]), the pose and velocity of every frame, the IMU bias (gyroscope and accelerator) and the extrinsic parameters are optimized together.

The state estimation can be thought as a Maximum A Posteriori (MAP) problem [8]. The estimation of the state is equal to calculating the conditional probability distribution of state quantities under conditions of known observations:

$$P(\mathbf{x}|\mathbf{z}) \quad (34)$$

According to the Bayesian rule, we have

$$P(\mathbf{x}|\mathbf{z}) = \frac{P(\mathbf{z}|\mathbf{x})P(\mathbf{x})}{P(\mathbf{z})} \propto P(\mathbf{z}|\mathbf{x})P(\mathbf{x}) \quad (35)$$

where $P(\mathbf{x}|\mathbf{z})$ is the posterior probability, $P(\mathbf{x})$ is the priori probability, $P(\mathbf{z}|\mathbf{x})$ is the likelihood probability. It is difficult to calculate the posterior probability distribution directly. However, it is feasible to find an optimal state estimation which maximizes the posterior probability. In most cases, we do not have any priori information about the state of the system. So, we have

$$\mathbf{x}^* = \arg \max P(\mathbf{x}|\mathbf{z}) \propto \arg \max P(\mathbf{z}|\mathbf{x})P(\mathbf{x}) \propto \arg \max P(\mathbf{z}|\mathbf{x}) \quad (36)$$

The problem has become to find a state of the system that can produce the observations most probably.

We assume the uncertainty of measurement is Gaussian distributed, namely, $\mathbf{z} \sim N(\bar{\mathbf{z}}, \mathbf{Q})$. Then, the negative log-likelihood of (36) can be written as

$$\mathbf{x}^* = \arg \max P(\mathbf{z}|\mathbf{x}) = \arg \min \sum \|\mathbf{z} - h(\mathbf{x})\|_{\mathbf{Q}} \quad (37)$$

$h(\bullet)$ is a function of the state. $\|\bullet\|_{\mathbf{Q}}$ denotes the Mahalanobis norm.

NOTICE: Think about arbitrary dimension Gaussian distribution $\mathbf{x} \sim N(\boldsymbol{\mu}, \mathbf{Q})$, the probability density function of \mathbf{x} can be written as

$$P(\mathbf{x}) = \frac{1}{\sqrt{(2\pi)^N \det(\mathbf{Q})}} \exp\left(-\frac{1}{2}(\mathbf{x} - \boldsymbol{\mu})^T \mathbf{Q}^{-1}(\mathbf{x} - \boldsymbol{\mu})\right) \quad (38)$$

$$-\ln P(\mathbf{x}) = \ln \sqrt{(2\pi)^N \det(\mathbf{Q})} + \frac{1}{2}(\mathbf{x} - \boldsymbol{\mu})^T \mathbf{Q}^{-1}(\mathbf{x} - \boldsymbol{\mu}) \quad (39)$$

Since the first part in the left side does not contain \mathbf{x} , so to maximize $P(\mathbf{x})$ become to minimize the second part in the left side of (39).

In the VINS-Mono, the cost function can be written as

$$\min_{\boldsymbol{\chi}} \left\{ \|\mathbf{r}_p - \mathbf{J}_p \boldsymbol{\chi}\|_{\mathbf{P}_p} + \sum_{k \in \mathbf{B}} \|\mathbf{r}_B(\hat{\mathbf{z}}_{b_{k+1}}^{b_k}, \boldsymbol{\chi})\|_{\mathbf{P}_B} + \sum_{(l,j) \in \mathbf{C}} \|\mathbf{r}_C(\hat{\mathbf{z}}_l^{c_j}, \boldsymbol{\chi})\|_{\mathbf{P}_l^{c_j}} \right\} \quad (40)$$

where $(\mathbf{r}_p, \mathbf{J}_p)$ is the priori information from marginalization, \mathbf{r}_B is the residuals of the IMU measurements, \mathbf{B} is the set of all IMU measurements in the sliding window, \mathbf{r}_C is the residuals of the visual model, and \mathbf{C} is the set of features which have been observed at least two times in the sliding window.

The state estimation is converted to a nonlinear least square problem, and it can be solved by Gaussian-Newton or Levenberg-Marquardt approach.

We take the Gaussian-Newton approach for example and we consider a general optimization problem.

$$\chi = \underset{\mathbf{x}}{\operatorname{argmin}} \|f(\mathbf{x})\|_{\mathbf{P}} \quad (41)$$

where \mathbf{P} is the covariance matrix of the residuals. We take into account the first-order Taylor expansion of the cost function $f(\mathbf{x})$, then the problem become calculating the increment $\delta\mathbf{x}$.

$$\begin{aligned} \delta\mathbf{x}^* &= \underset{\delta\mathbf{x}}{\operatorname{argmin}} \|f(\mathbf{x}) + \mathbf{J}(\mathbf{x})\delta\mathbf{x}\|_{\mathbf{P}} \\ \|f(\mathbf{x}) + \mathbf{J}(\mathbf{x})\delta\mathbf{x}\|_{\mathbf{P}} &= (f(\mathbf{x}) + \mathbf{J}(\mathbf{x})\delta\mathbf{x})^T \mathbf{P}^{-1} (f(\mathbf{x}) + \mathbf{J}(\mathbf{x})\delta\mathbf{x}) \\ &= f(\mathbf{x})^T \mathbf{P}^{-1} f(\mathbf{x}) + 2\mathbf{J}(\mathbf{x})^T \mathbf{P}^{-1} f(\mathbf{x})\delta\mathbf{x} + \delta\mathbf{x}^T \mathbf{J}(\mathbf{x})^T \mathbf{P}^{-1} \mathbf{J}(\mathbf{x})\delta\mathbf{x} \end{aligned} \quad (42)$$

Calculate the derivative of the function in (42) and let it equal to zero, we have

$$\begin{aligned} \mathbf{J}(\mathbf{x})^T \mathbf{P}^{-1} \mathbf{J}(\mathbf{x})\delta\mathbf{x} &= -\mathbf{J}(\mathbf{x})^T \mathbf{P}^{-1} f(\mathbf{x}) \\ \mathbf{H}\delta\mathbf{x} &= \mathbf{b} \end{aligned} \quad (43)$$

4.2 IMU Model

From (5), we can write the residuals of IMU measurements as follow,

$$\mathbf{r}_B(\hat{\mathbf{z}}_{b_{k+1}}^{b_k}, \chi) = \begin{bmatrix} \delta\alpha_{b_{k+1}}^{b_k} \\ \delta\theta_{b_{k+1}}^{b_k} \\ \delta\beta_{b_{k+1}}^{b_k} \\ \delta\mathbf{b}_a \\ \delta\mathbf{b}_g \end{bmatrix} = \begin{bmatrix} \mathbf{R}_w^{b_k} (\mathbf{p}_{b_{k+1}}^w - \mathbf{p}_{b_k}^w - \mathbf{v}_{b_k}^w \Delta t_k + \frac{1}{2} \mathbf{g}^w \Delta t_k^2) - \hat{\alpha}_{b_{k+1}}^{b_k} \\ 2 \left[(\hat{\gamma}_{b_{k+1}}^{b_k})^{-1} \otimes (\mathbf{q}_{b_k}^w)^{-1} \otimes \mathbf{q}_{b_{k+1}}^w \right]_{xyz} \\ \mathbf{R}_w^{b_k} (\mathbf{v}_{b_{k+1}}^w - \mathbf{v}_{b_k}^w + \mathbf{g}^w \Delta t_k) - \hat{\beta}_{b_{k+1}}^{b_k} \\ \mathbf{b}_{a_{k+1}} - \mathbf{b}_{a_k} \\ \mathbf{b}_{g_{k+1}} - \mathbf{b}_{g_k} \end{bmatrix} \quad (44)$$

For IMU model, the optimization variables are

$$\begin{bmatrix} \mathbf{p}_{b_k}^w & \mathbf{q}_{b_k}^w \end{bmatrix} \begin{bmatrix} \mathbf{v}_{b_k}^w & \mathbf{b}_{a_k} & \mathbf{b}_{g_k} \end{bmatrix} \begin{bmatrix} \mathbf{p}_{b_{k+1}}^w & \mathbf{q}_{b_{k+1}}^w \end{bmatrix} \begin{bmatrix} \mathbf{v}_{b_{k+1}}^w & \mathbf{b}_{a_{k+1}} & \mathbf{b}_{g_{k+1}} \end{bmatrix} \quad (45)$$

It is consistent with the code implementation. The dimension of the state vectors above are <7, 9, 7, 9> respectively.

NOTICE: In the state vector, we use the quaternion to represent the attitude of the vehicle. It is not convenient to calculate the Jacobian w.r.t the attitude in quaternion. In addition, we know that the degrees of attitude is three while there are four variables in the quaternion which can overparameterize the problem. So we use Lie-algebra $so(3)$ (namely, rotation vector) to perform perturbation analysis and iterative optimization when consider the attitude errors. We calculate the increment of attitude in $so(3)$, then we update the states by the quaternion of the attitude increment. This is implemented by instantiating “LocalParameterization” in ceres solver [9]. The authors in [1] define the dimension of attitude parameter as four, so the dimensions of Jacobian matrix should be $\langle 15 \times 7, 15 \times 9, 15 \times 7, 15 \times 9 \rangle$. Therefore the last row of $\mathbf{J}[0]$ and $\mathbf{J}[2]$ is zero, for a simple expression, we only write the left six rows of them (see (46) and (48)). The vision model is the same.

The explanation of the attitude perturbation analysis is shown in Appendix A. We perform perturbation analysis for (44), and the Jacobian matrix can be written as follows. The proofs can be found in Appendix B.

$$\mathbf{J}[0]_{15 \times 6} = \frac{\partial \mathbf{r}_B(\hat{\mathbf{z}}_{b_{k+1}}^{b_k}, \chi)}{\partial \begin{bmatrix} \mathbf{p}_{b_k}^w & \mathbf{q}_{b_k}^w \end{bmatrix}} = \begin{bmatrix} -\mathbf{R}_w^{b_k} \left[\mathbf{R}_w^{b_k} (\mathbf{p}_{b_{k+1}}^w - \mathbf{p}_{b_k}^w - \mathbf{v}_{b_k}^w \Delta t_k + \frac{1}{2} \mathbf{g}^w \Delta t_k^2) \right] \times \\ \mathbf{0} & -R[\gamma_{b_{k+1}}^{b_k}] L \left[(\mathbf{q}_{b_{k+1}}^w)^{-1} \otimes \mathbf{q}_{b_k}^w \right]_{3 \times 3} \\ \mathbf{0} & \left[\mathbf{R}_w^{b_k} (\mathbf{p}_{b_{k+1}}^w - \mathbf{p}_{b_k}^w + \mathbf{g}^w \Delta t_k) \right] \times \\ \mathbf{0} & \mathbf{0} \\ \mathbf{0} & \mathbf{0} \end{bmatrix} \quad (46)$$

$$\mathbf{J}[1]_{15 \times 9} = \frac{\partial \mathbf{r}_B(\hat{\mathbf{z}}_{b_{k+1}}^{b_k}, \chi)}{\partial \begin{bmatrix} \mathbf{v}_{b_k}^w & \mathbf{b}_{ak} & \mathbf{b}_{gk} \end{bmatrix}} = \begin{bmatrix} -\mathbf{R}_w^{b_k} \Delta t_k & -\mathbf{J}_{b_a}^\alpha & -\mathbf{J}_{b_g}^\alpha & \\ \mathbf{0} & \mathbf{0} & -R \left[(\hat{\gamma}_{b_{k+1}}^{b_k})^{-1} \otimes (\mathbf{q}_{b_k}^w)^{-1} \otimes \mathbf{q}_{b_{k+1}}^w \right]_{3 \times 3} & \mathbf{J}_{b_g}^\gamma \\ -\mathbf{R}_w^{b_k} & -\mathbf{J}_{b_a}^\beta & -\mathbf{J}_{b_g}^\beta & \\ \mathbf{0} & -\mathbf{I} & \mathbf{0} & \\ \mathbf{0} & \mathbf{0} & -\mathbf{I} & \end{bmatrix} \quad (47)$$

$$\mathbf{J}[2]_{15 \times 6} = \frac{\partial \mathbf{r}_B(\hat{\mathbf{z}}_{b_{k+1}}^{b_k}, \chi)}{\partial \begin{bmatrix} \mathbf{p}_{b_{k+1}}^w & \mathbf{q}_{b_{k+1}}^w \end{bmatrix}} = \begin{bmatrix} \mathbf{R}_w^{b_k} & \mathbf{0} \\ \mathbf{0} & L \left[(\hat{\gamma}_{b_{k+1}}^{b_k})^{-1} \otimes (\mathbf{q}_{b_k}^w)^{-1} \otimes \mathbf{q}_{b_{k+1}}^w \right] \\ \mathbf{0} & \mathbf{0} \\ \mathbf{0} & \mathbf{0} \\ \mathbf{0} & \mathbf{0} \end{bmatrix} \quad (48)$$

$$\mathbf{J}[3]_{15 \times 9} = \frac{\partial \mathbf{r}_B(\hat{\mathbf{z}}_{b_{k+1}}^{b_k}, \boldsymbol{\chi})}{\partial \begin{bmatrix} \mathbf{v}_{b_{k+1}}^w & \mathbf{b}_{ak+1} & \mathbf{b}_{gk+1} \end{bmatrix}} = \begin{bmatrix} \mathbf{0} & \mathbf{0} & \mathbf{0} \\ \mathbf{0} & \mathbf{0} & \mathbf{0} \\ \mathbf{R}_w^{b_k} & \mathbf{0} & \mathbf{0} \\ \mathbf{0} & \mathbf{I} & \mathbf{0} \\ \mathbf{0} & \mathbf{0} & \mathbf{I} \end{bmatrix} \quad (49)$$

4.3 Vision Model

Considering the l^{th} feature which is firstly observed in i^{th} image, the residual for the observation in the j^{th} image can be written as

$$\begin{aligned} \hat{\mathbf{P}}_l^{c_j} &= \boldsymbol{\pi}_c^{-1} \begin{bmatrix} \hat{\mathbf{u}}_l^{c_j} \\ \hat{\mathbf{v}}_l^{c_j} \end{bmatrix} \\ \tilde{\mathbf{P}}_l^{c_j} &= \mathbf{R}_b^c \left\{ \mathbf{R}_{b_j}^{b_j} \left[\mathbf{R}_{b_i}^w \left(\mathbf{R}_c^b \frac{1}{\lambda_l} \boldsymbol{\pi}_c^{-1} \begin{bmatrix} \hat{\mathbf{u}}_l^{c_i} \\ \hat{\mathbf{v}}_l^{c_i} \end{bmatrix} + \mathbf{P}_c^b \right) + \mathbf{P}_{b_i}^w \right] + \mathbf{P}_w^{b_j} \right\} + \mathbf{P}_b^{c_j} \\ &= \mathbf{R}_b^c \left\{ \mathbf{R}_w^{b_j} \left[\mathbf{R}_{b_i}^w \left(\mathbf{R}_c^b \frac{1}{\lambda_l} \boldsymbol{\pi}_c^{-1} \begin{bmatrix} \hat{\mathbf{u}}_l^{c_i} \\ \hat{\mathbf{v}}_l^{c_i} \end{bmatrix} + \mathbf{P}_c^b \right) + \mathbf{P}_{b_i}^w - \mathbf{P}_{b_j}^w \right] - \mathbf{P}_c^b \right\} \\ r_C(\hat{\mathbf{z}}_l^{c_j}, \boldsymbol{\chi}) &= [\mathbf{b}_1, \mathbf{b}_2]^T \cdot \left(\frac{\tilde{\mathbf{P}}_l^{c_j}}{\|\tilde{\mathbf{P}}_l^{c_j}\|} - \hat{\mathbf{P}}_l^{c_j} \right) \\ or \\ r_C(\hat{\mathbf{z}}_l^{c_j}, \boldsymbol{\chi}) &= \left(\frac{\tilde{\mathbf{P}}_l^{c_j}}{\tilde{\mathbf{P}}_l^{c_j} [2]} - \hat{\mathbf{P}}_l^{c_j} \right)_{head 2 \times 1} \end{aligned} \quad (50)$$

let

$$\bar{\mathbf{P}}_l^{c_i} = \boldsymbol{\pi}_c^{-1} \begin{bmatrix} \hat{\mathbf{u}}_l^{c_i} \\ \hat{\mathbf{v}}_l^{c_i} \end{bmatrix} \quad (51)$$

where $\boldsymbol{\pi}_c^{-1}$ is the back projection model which outputs the correspondence **normalized vector** in 3D space(see “projection_factor.cpp” in the code), $\begin{bmatrix} \hat{\mathbf{u}}_l^{c_i}, \hat{\mathbf{v}}_l^{c_i} \end{bmatrix}$ is the first observation of the l^{th} feature in the i^{th} image, $\begin{bmatrix} \hat{\mathbf{u}}_l^{c_j}, \hat{\mathbf{v}}_l^{c_j} \end{bmatrix}$ is the observation of the l^{th} feature in the j^{th} image. The

authors project the residual vector onto the tangent plane. $[\mathbf{b}_1, \mathbf{b}_2]$ are two arbitrarily selected

orthogonal bases which span the tangent plane of $\hat{\mathbf{P}}_l^{c_j}$.

NOTE: The second equation of (50) can be derived by the following equations.

$$\begin{aligned}\mathbf{R}_b^w \mathbf{P}^b + \mathbf{P}_b^w &= \mathbf{P}^w \\ \mathbf{P}_w^b &= -\mathbf{R}_w^b \mathbf{P}_b^w\end{aligned}\tag{52}$$

For Vision model, the optimization variables are

$$[\mathbf{p}_{b_i}^w \quad \mathbf{q}_{b_i}^w][\mathbf{p}_{b_j}^w \quad \mathbf{q}_{b_j}^w][\mathbf{p}_c^b \quad \mathbf{q}_c^b], \lambda_l\tag{53}$$

The Jacobian matrix can be calculated by the chain rule,

$$\frac{\partial \mathbf{r}_C}{\partial \mathbf{x}} = \frac{\partial \mathbf{r}_C}{\partial \tilde{\mathbf{P}}_l^{c_j}} \bullet \frac{\partial \tilde{\mathbf{P}}_l^{c_j}}{\partial \mathbf{x}}\tag{54}$$

For general form, we have

$$\frac{\partial \mathbf{r}_C}{\partial \tilde{\mathbf{P}}_l^{c_j}} = \begin{bmatrix} \frac{1}{z_l^{c_j}} & 0 & -\frac{x_l^{c_j}}{(z_l^{c_j})^2} \\ 0 & \frac{1}{z_l^{c_j}} & -\frac{y_l^{c_j}}{(z_l^{c_j})^2} \end{bmatrix}\tag{55}$$

For the tangent space form, we have

$$\begin{aligned}
\frac{\partial \mathbf{r}_c}{\partial \tilde{\mathbf{P}}_l^{c_j}} &= [\mathbf{b}_1, \mathbf{b}_2]^T \cdot \frac{\partial \left(\frac{\tilde{\mathbf{P}}_l^{c_j}}{\|\tilde{\mathbf{P}}_l^{c_j}\|} - \hat{\mathbf{P}}_l^{c_j} \right)}{\partial \tilde{\mathbf{P}}_l^{c_j}} \\
&= \frac{\partial \frac{\tilde{\mathbf{P}}_l^{c_j}}{\|\tilde{\mathbf{P}}_l^{c_j}\|}}{\partial \tilde{\mathbf{P}}_l^{c_j}} = \frac{1}{\|\tilde{\mathbf{P}}_l^{c_j}\|} \mathbf{I} - \frac{\tilde{\mathbf{P}}_l^{c_j} \frac{\partial \|\tilde{\mathbf{P}}_l^{c_j}\|}{\partial \tilde{\mathbf{P}}_l^{c_j}}}{\|\tilde{\mathbf{P}}_l^{c_j}\|^2} \\
&= \begin{bmatrix} \frac{1}{\|\tilde{\mathbf{P}}_l^{c_j}\|} - \frac{x^2}{\|\tilde{\mathbf{P}}_l^{c_j}\|^3} & -\frac{xy}{\|\tilde{\mathbf{P}}_l^{c_j}\|^3} & -\frac{xz}{\|\tilde{\mathbf{P}}_l^{c_j}\|^3} \\ -\frac{xy}{\|\tilde{\mathbf{P}}_l^{c_j}\|^3} & \frac{1}{\|\tilde{\mathbf{P}}_l^{c_j}\|} - \frac{y^2}{\|\tilde{\mathbf{P}}_l^{c_j}\|^3} & -\frac{yz}{\|\tilde{\mathbf{P}}_l^{c_j}\|^3} \\ -\frac{xz}{\|\tilde{\mathbf{P}}_l^{c_j}\|^3} & -\frac{yz}{\|\tilde{\mathbf{P}}_l^{c_j}\|^3} & \frac{1}{\|\tilde{\mathbf{P}}_l^{c_j}\|} - \frac{z^2}{\|\tilde{\mathbf{P}}_l^{c_j}\|^3} \end{bmatrix} \\
&\quad \left(\text{let } \tilde{\mathbf{P}}_l^{c_j} = [x \ y \ z]^T \right)
\end{aligned} \tag{56}$$

For $\frac{\partial \tilde{\mathbf{P}}_l^{c_j}}{\partial \mathbf{x}}$, we have the following equations, and the proofs can be found in Appendix C.

$$\mathbf{J}[0]_{3 \times 6} = \frac{\partial \tilde{\mathbf{P}}_l^{c_j}}{\partial \begin{bmatrix} \mathbf{p}_{b_i}^w & \mathbf{q}_{b_i}^w \end{bmatrix}} = \begin{bmatrix} \mathbf{R}_b^c \mathbf{R}_w^{b_j} & -\mathbf{R}_b^c \mathbf{R}_w^{b_j} \mathbf{R}_{b_i}^w \left[\left(\frac{1}{\lambda_l} \mathbf{R}_c^b \bar{\mathbf{P}}_l^{c_i} + \mathbf{P}_c^b \right) \times \right] \end{bmatrix} \tag{57}$$

$$\mathbf{J}[1]_{3 \times 6} = \frac{\partial \tilde{\mathbf{P}}_l^{c_j}}{\partial \begin{bmatrix} \mathbf{p}_{b_j}^w & \mathbf{q}_{b_j}^w \end{bmatrix}} = \begin{bmatrix} -\mathbf{R}_b^c \mathbf{R}_w^{b_j} & \mathbf{R}_b^c \left\{ \left[\mathbf{R}_w^{b_j} \left(\mathbf{R}_{b_i}^w \left(\mathbf{R}_c^b \frac{1}{\lambda_l} \bar{\mathbf{P}}_l^{c_i} \right) + \mathbf{P}_{b_i}^w - \mathbf{P}_{b_j}^w \right) \right] \times \right\} \end{bmatrix} \tag{58}$$

$$\begin{aligned}
\mathbf{J}[2]_{3 \times 6} &= \frac{\partial \tilde{\mathbf{P}}_l^{c_j}}{\partial \begin{bmatrix} \mathbf{p}_c^b & \mathbf{q}_c^b \end{bmatrix}} = \\
&\begin{bmatrix} \mathbf{R}_b^c \left(\mathbf{R}_w^{b_j} \mathbf{R}_{b_i}^w - \mathbf{I} \right) \left[\mathbf{R}_b^c \left(\mathbf{R}_w^{b_j} \left[\mathbf{R}_{b_i}^w \mathbf{P}_c^b + \mathbf{P}_{b_i}^w - \mathbf{P}_{b_j}^w \right] - \mathbf{P}_c^b \right) \right] \times + \\ \left(\mathbf{R}_b^c \mathbf{R}_w^{b_j} \mathbf{R}_{b_i}^w \mathbf{R}_c^b \frac{1}{\lambda_l} \bar{\mathbf{P}}_l^{c_i} \right) \times - \mathbf{R}_b^c \mathbf{R}_w^{b_j} \mathbf{R}_{b_i}^w \mathbf{R}_c^b \left(\frac{1}{\lambda_l} \bar{\mathbf{P}}_l^{c_i} \times \right) \end{bmatrix} \tag{59}
\end{aligned}$$

$$\mathbf{J}[3]_{3 \times 1} = \frac{\partial \tilde{\mathbf{P}}_l^{c_j}}{\partial \lambda_l} = \left[-\frac{1}{\lambda_l^2} \mathbf{R}_b^c \mathbf{R}_w^{b_j} \mathbf{R}_{b_i}^w \mathbf{R}_c^b \bar{\mathbf{P}}_l^{c_i} \right] \tag{60}$$

V. Marginalization

Since the number of states increase along with the time, the computational complexity will increase quadratically accordingly. In order to reduce compute amount without loss of information, we perform marginalization procedure to convert the previous measurements into a prior term. The set of states to be marginalized is denoted as χ_m and the set of remaining states is denoted as χ_r . According to (43), we rearrange the states' order and get the following equation

$$\begin{bmatrix} \mathbf{H}_{mm} & \mathbf{H}_{mr} \\ \mathbf{H}_{rm} & \mathbf{H}_{rr} \end{bmatrix} \begin{bmatrix} \delta \mathbf{x}_m \\ \delta \mathbf{x}_r \end{bmatrix} = \begin{bmatrix} \mathbf{b}_m \\ \mathbf{b}_r \end{bmatrix} \quad (61)$$

Then we perform the Schur complement to carry out the marginalization [10, 11] as follows

$$\begin{bmatrix} \mathbf{I} & \mathbf{0} \\ -\mathbf{H}_{rm} \mathbf{H}_{mm}^{-1} & \mathbf{I} \end{bmatrix} \begin{bmatrix} \mathbf{H}_{mm} & \mathbf{H}_{mr} \\ \mathbf{H}_{rm} & \mathbf{H}_{rr} \end{bmatrix} \begin{bmatrix} \delta \mathbf{x}_m \\ \delta \mathbf{x}_r \end{bmatrix} = \begin{bmatrix} \mathbf{I} & \mathbf{0} \\ -\mathbf{H}_{rm} \mathbf{H}_{mm}^{-1} & \mathbf{I} \end{bmatrix} \begin{bmatrix} \mathbf{b}_m \\ \mathbf{b}_r \end{bmatrix} \quad (62)$$

$$\begin{bmatrix} \mathbf{H}_{mm} & \mathbf{H}_{mr} \\ \mathbf{0} & \underbrace{-\mathbf{H}_{rm} \mathbf{H}_{mm}^{-1} \mathbf{H}_{mr} + \mathbf{H}_{rr}}_{\mathbf{H}_p} \end{bmatrix} \begin{bmatrix} \delta \mathbf{x}_m \\ \delta \mathbf{x}_r \end{bmatrix} = \begin{bmatrix} \mathbf{b}_m \\ \underbrace{-\mathbf{H}_{rm} \mathbf{H}_{mm}^{-1} \mathbf{b}_m + \mathbf{b}_r}_{\mathbf{b}_p} \end{bmatrix}$$

$$\left(-\mathbf{H}_{rm} \mathbf{H}_{mm}^{-1} \mathbf{H}_{mr} + \mathbf{H}_{rr} \right) \delta \mathbf{x}_r = -\mathbf{H}_{rm} \mathbf{H}_{mm}^{-1} \mathbf{b}_m + \mathbf{b}_r \quad (63)$$

Denote that we keep states from instant m to instant n in the sliding window. The states before m are marginalized out and converted to a prior term. Therefore, the MAP problem is written as [11],

$$\chi_{m:n}^* = \arg \min_{\chi_{m:n}} \sum_{t=m}^n \sum_{k \in \mathbf{S}} \left\{ \left\| \mathbf{z}_t^k - h_t^k(\chi_{m:n}) \right\|_{\Omega_t^k}^2 + (\mathbf{H}_p \delta \mathbf{x}_r - \mathbf{b}_p) \right\} \quad (64)$$

Where \mathbf{S} is the set of measurements.

VI. Global Optimization in VINS-Fusion

A general optimization based framework for global pose estimation is proposed in [12], which is an extension of [1]. Local estimation from VIO/VO is fused with global sensors in a pose graph optimization. Within the optimization, the transformation from local frame to global frame is estimated, so the local state can be aligned into the global coordinate system. The illustration of the global pose graph structure is shown in Figure 4. The state vector to be estimated in global optimization is shown in (65).

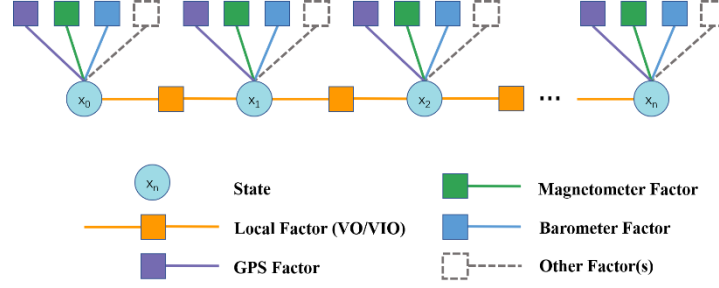


Figure 4 Illustration of the global pose graph structure

$$\chi = [\mathbf{q}_i^G, \mathbf{P}_i^G, \dots, \mathbf{q}_n^G, \mathbf{P}_n^G] \quad (65)$$

Every node contains the pose of the vehicle in the global frame (Here is the GPS frame), while the edge between two consecutive nodes is a local constraint from VIO/VO estimation. The local pose and global pose of one node can be written as a combination of rotation and translation

$$\begin{aligned} \mathbf{T}_i^l &= [\mathbf{R}_i^l \quad \mathbf{P}_i^l] \\ \mathbf{T}_i^G &= [\mathbf{R}_i^G \quad \mathbf{P}_i^G] \end{aligned} \quad (66)$$

where i is the i^{th} node, l is the local reference frame, G is the global reference frame, \mathbf{R} , \mathbf{T} is the rotation and translation from body frame to reference frame, respectively. Given two consecutive nodes i and j , the relative transformation can be derived from local pose and global pose respectively. In the code, the authors set the first GPS point as the origin and subsequently set the ENU coordinate system as global frame.

$$\mathbf{T}_{j-l}^i = \begin{bmatrix} \mathbf{R}_i^l & \mathbf{P}_i^l \\ 0 & 1 \end{bmatrix}^{-1} \begin{bmatrix} \mathbf{R}_j^l & \mathbf{P}_j^l \\ 0 & 1 \end{bmatrix} = \begin{bmatrix} \mathbf{R}_{j-l}^i & \mathbf{P}_{ij-l}^i \\ 0 & 1 \end{bmatrix} \quad (67)$$

$$\mathbf{T}_{j-G}^i = \begin{bmatrix} \mathbf{R}_G^i \mathbf{R}_j^G & \mathbf{R}_G^i (\mathbf{P}_j^G - \mathbf{P}_i^G) \\ 0 & 1 \end{bmatrix} = \begin{bmatrix} \mathbf{R}_{j-G}^i & \mathbf{P}_{ij-G}^i \\ 0 & 1 \end{bmatrix} \quad (68)$$

Then, the residuals can be written as

$$\begin{bmatrix} \delta \mathbf{P}_{ij} \\ \delta \boldsymbol{\theta}_{ij} \end{bmatrix} = \begin{bmatrix} \mathbf{P}_{ij-G}^i - \mathbf{P}_{ij-l}^i \\ 2(\mathbf{q}_{j-l}^i)^{-1} \mathbf{q}_{j-G}^i \end{bmatrix} \quad (69)$$

For GPS position constraint, we have

$$\delta \mathbf{P}_i = [\mathbf{P}_{i_estimation}^G - \mathbf{P}_{i_measurement}^G] \quad (70)$$

The standard deviation (std) of global position error can be obtained from GPS positioning algorithm directly. In the code¹, the std of local position and rotation are fixed, 0.1 m for position error std, 0.01 rad for rotation error std, respectively.

The two factors are jointly optimized by ceres solver, since the pose graph is quite sparse, the authors keep a huge window to get accurate and globally drift-free pose estimation(not implemented in the code). Although many nodes are optimized, the transformation between local frame and global frame is updated only by the global pose of the last node. As far as I concerned, all the nodes should be taken into account to reduce the effect of gross errors.

However, the time synchronization between VIO and GPS measurements is not elegantly handled in the code, which may introduce non-trivial pose error. Moreover, the GPS observations are not used to correct the accumulated error in VIO/VO.

VII. Appendix

A. Attitude Perturbation

In most optimization problems, we calculate the Jacobian of residuals w.r.t. the variables at first. Then we use the output increment to update the state of the vehicle. So the way that we compute the Jacobian is relative to the way we update the state of body.

There are many attitude representations to parameterize the attitude of vehicles. Their definitions and the conversions from one form to another can be found in [5, 13]

It is worth mentioning that the rotation vector and rotation matrix correspond with the Lie-algebra $so(3)$ and Lie-group $SO(3)$, respectively.

The authors in [1] use quaternion to represent the attitude of the vehicle, and use the rotation matrix to represent the transformation between two coordinates. The authors define the update way of the vehicle attitude as (see “pose_local_parameterization.cpp” in the code)

$$\mathbf{q}_{b'}^w = \mathbf{q}_b^w \delta \mathbf{q}_{b'}^b \quad (71)$$

where, \mathbf{q}_b^w is the vehicle attitude derived from the dynamic evolution function, $\delta \mathbf{q}_{b'}^b$

is the increment calculated by the nonlinear optimization. $\mathbf{q}_{b'}^w$ is the attitude after optimization.

So the perturbation should be the attitude error in b-frame (from current b to b') when we perform perturbation analysis on the residual function. For example,

$$\begin{aligned} \mathbf{R}_b^w(\delta \theta) &= \mathbf{R}_b^w \exp(\delta \theta_{b'}^b) \approx \mathbf{R}_b^w (\mathbf{I} + \delta \theta_{b'}^b \times) \\ \mathbf{R}_w^b(\delta \theta) &= \exp(\delta \theta_{b'}^b) \mathbf{R}_w^b \approx (\mathbf{I} - \delta \theta_{b'}^b \times) \mathbf{R}_w^b \end{aligned} \quad (72)$$

¹ <https://github.com/HKUST-Aerial-Robotics/VINS-Fusion>

Where, $\mathbf{R}_b^w(\delta\theta)$ and $\mathbf{R}_w^b(\delta\theta)$ are the attitudes with perturbation, $\delta\theta_b^b$ is the rotation vector corresponding to the attitude perturbation.

B. Proofs of The Jacobian of The IMU Model

Given (71) and (72), we have

1) $\mathbf{J}[0]$:

$$\begin{aligned} \frac{\partial \delta \alpha_{b_{k+1}}^{b_k}}{\partial \mathbf{p}_{b_k}^w} &= \lim_{\delta \mathbf{p}_{b_k}^w \rightarrow 0} \frac{\mathbf{R}_w^{b_k}(\mathbf{p}_{b_{k+1}}^w - (\mathbf{p}_{b_k}^w + \delta \mathbf{p}_{b_k}^w) - \mathbf{v}_{b_k}^w \Delta t_k + \frac{1}{2} \mathbf{g}^w \Delta t_k^2) - \hat{\alpha}_{b_{k+1}}^{b_k} - \delta \alpha_{b_{k+1}}^{b_k}}{\delta \mathbf{p}_{b_k}^w} \\ &= -\mathbf{R}_w^{b_k} \end{aligned} \quad (73)$$

Perform the Lie-algebra left multiplication perturbation model [8], we have

$$\begin{aligned} \frac{\partial \delta \alpha_{b_{k+1}}^{b_k}}{\partial \mathbf{q}_{b_k}^w} &= \lim_{\delta \theta_{b_k}^{b_k} \rightarrow 0} \frac{\exp(\delta \theta_{b_k}^{b_k}) \mathbf{R}_w^{b_k} \left(\mathbf{p}_{b_{k+1}}^w - \mathbf{p}_{b_k}^w - \mathbf{v}_{b_k}^w \Delta t_k + \frac{1}{2} \mathbf{g}^w \Delta t_k^2 \right) - \mathbf{R}_w^{b_k} \left(\mathbf{p}_{b_{k+1}}^w - \mathbf{p}_{b_k}^w - \mathbf{v}_{b_k}^w \Delta t_k + \frac{1}{2} \mathbf{g}^w \Delta t_k^2 \right)}{\partial \theta_{b_k}^w} \\ &= \lim_{\delta \theta_{b_k}^{b_k} \rightarrow 0} \frac{\left((\mathbf{I} - \delta \theta_{b_k}^{b_k} \times) \mathbf{R}_w^{b_k} - \mathbf{R}_w^{b_k} \right) \left(\mathbf{p}_{b_{k+1}}^w - \mathbf{p}_{b_k}^w - \mathbf{v}_{b_k}^w \Delta t_k + \frac{1}{2} \mathbf{g}^w \Delta t_k^2 \right)}{\partial \theta_{b_k}^w} \\ &= \left[\mathbf{R}_w^{b_k} (\mathbf{p}_{b_{k+1}}^w - \mathbf{p}_{b_k}^w - \mathbf{v}_{b_k}^w \Delta t_k + \frac{1}{2} \mathbf{g}^w \Delta t_k^2) \right] \times \end{aligned} \quad (74)$$

One thing that we must pay attention to is that the cross production does not confirm the associative law, namely

$$\mathbf{A}(\mathbf{p} \times) \mathbf{B} \neq (\mathbf{A} \mathbf{p}) \times \mathbf{B} \quad (75)$$

From [5], we know

$$\delta \mathbf{q} \approx \begin{bmatrix} 1 \\ \frac{1}{2} \delta \theta \end{bmatrix} \quad (76)$$

$$\mathbf{q}^* = \begin{bmatrix} q_w \\ -\mathbf{q}_v \end{bmatrix} \quad (77)$$

$$(\mathbf{p} \otimes \mathbf{q})^* = \mathbf{q}^* \otimes \mathbf{p}^*$$

For unit quaternion, we have

$$\mathbf{q}^{-1} = \mathbf{q}^* \quad (78)$$

$$L[\mathbf{q}^{-1}]_{3 \times 3} = R[\mathbf{q}]_{3 \times 3} \quad (79)$$

where, $L[\bullet]$ and $R[\bullet]$ are respectively the left- and right- quaternion-product matrices, $[\bullet]_{3 \times 3}$ is the 3×3 block at the right-bottom of the matrix.

$$\begin{aligned} \frac{\partial \delta \boldsymbol{\theta}_{b_{k+1}}^{b_k}}{\partial \mathbf{q}_{b_k}^w} &= \lim_{\delta \boldsymbol{\theta}_{b_k}^w \rightarrow 0} \frac{2 \left[\left(\hat{\boldsymbol{\gamma}}_{b_{k+1}}^{b_k} \right)^{-1} \otimes \left(\mathbf{q}_{b_k}^w \otimes \begin{bmatrix} 1 \\ \frac{1}{2} \delta \boldsymbol{\theta}_{b_k}^w \end{bmatrix} \right)^{-1} \otimes \mathbf{q}_{b_{k+1}}^w \right]_{xyz} - 2 \left[\left(\hat{\boldsymbol{\gamma}}_{b_{k+1}}^{b_k} \right)^{-1} \otimes \left(\mathbf{q}_{b_k}^w \otimes \begin{bmatrix} 1 \\ 0 \end{bmatrix} \right)^{-1} \otimes \mathbf{q}_{b_{k+1}}^w \right]_{xyz}}{\delta \boldsymbol{\theta}_{b_k}^w} \\ &\approx \lim_{\delta \boldsymbol{\theta}_{b_k}^w \rightarrow 0} \frac{2 \left[\left(\hat{\boldsymbol{\gamma}}_{b_{k+1}}^{b_k} \right)^{-1} \otimes \begin{bmatrix} 1 \\ -\frac{1}{2} \delta \boldsymbol{\theta}_{b_k}^w \end{bmatrix} \otimes \left(\mathbf{q}_{b_k}^w \right)^{-1} \otimes \mathbf{q}_{b_{k+1}}^w \right]_{xyz} - 2 \left[\left(\hat{\boldsymbol{\gamma}}_{b_{k+1}}^{b_k} \right)^{-1} \otimes \begin{bmatrix} 1 \\ 0 \end{bmatrix} \otimes \left(\mathbf{q}_{b_k}^w \right)^{-1} \otimes \mathbf{q}_{b_{k+1}}^w \right]_{xyz}}{\delta \boldsymbol{\theta}_{b_k}^w} \\ &= \lim_{\delta \boldsymbol{\theta}_{b_k}^w \rightarrow 0} \frac{2L \left[\left(\hat{\boldsymbol{\gamma}}_{b_{k+1}}^{b_k} \right)^{-1} \right] R \left[\left(\mathbf{q}_{b_k}^w \right)^{-1} \otimes \mathbf{q}_{b_{k+1}}^w \right] \begin{bmatrix} 0 \\ -\frac{1}{2} \delta \boldsymbol{\theta}_{b_k}^w \end{bmatrix}}{\delta \boldsymbol{\theta}_{b_k}^w} \\ &= -L \left[\left(\hat{\boldsymbol{\gamma}}_{b_{k+1}}^{b_k} \right)^{-1} \right] R \left[\left(\mathbf{q}_{b_k}^w \right)^{-1} \otimes \mathbf{q}_{b_{k+1}}^w \right]_{3 \times 3} \\ &= -L \left[\left(\mathbf{q}_{b_{k+1}}^w \right)^{-1} \otimes \mathbf{q}_{b_k}^w \right] R \left[\hat{\boldsymbol{\gamma}}_{b_{k+1}}^{b_k} \right]_{3 \times 3} \end{aligned} \quad (80)$$

As the same as (74), we have

$$\frac{\partial \delta \boldsymbol{\beta}_{b_{k+1}}^{b_k}}{\partial \mathbf{q}_{b_k}^w} = \left[\mathbf{R}_{b_k}^{b_k} (\mathbf{v}_{b_{k+1}}^w - \mathbf{v}_{b_k}^w + \mathbf{g}^w \Delta t_k) \right] \times \quad (81)$$

2) $\mathbf{J}[1]$:

$$\frac{\partial \delta \boldsymbol{\alpha}_{b_{k+1}}^{b_k}}{\partial \mathbf{v}_{b_k}^w} = \lim_{\delta \mathbf{v}_{b_k}^w \rightarrow 0} \frac{\mathbf{R}_{b_k}^{b_k} (\mathbf{p}_{b_{k+1}}^w - \mathbf{p}_{b_k}^w - (\mathbf{v}_{b_k}^w + \delta \mathbf{v}_{b_k}^w) \Delta t_k + \frac{1}{2} \mathbf{g}^w \Delta t_k^2) - \hat{\boldsymbol{\alpha}}_{b_{k+1}}^{b_k} - \delta \boldsymbol{\alpha}_{b_{k+1}}^{b_k}}{\delta \mathbf{v}_{b_k}^w} = -\mathbf{R}_{b_k}^{b_k} \Delta t_k \quad (82)$$

Given (20), we

$$\begin{aligned}
\frac{\partial \delta \alpha_{b_{k+1}}^{b_k}}{\partial \mathbf{b}_{ak}} &= \lim_{\delta \mathbf{b}_{ak} \rightarrow 0} \frac{-\left(\hat{\alpha}_{b_{k+1}}^{b_k} + \mathbf{J}_{b_a}^\alpha \delta b_{a_k}\right) + \hat{\alpha}_{b_{k+1}}^{b_k}}{\delta \mathbf{b}_{ak}} = -\mathbf{J}_{b_a}^\alpha \\
\frac{\partial \delta \alpha_{b_{k+1}}^{b_k}}{\partial \mathbf{b}_{gk}} &= \lim_{\delta \mathbf{b}_{gk} \rightarrow 0} \frac{-\left(\hat{\alpha}_{b_{k+1}}^{b_k} + \mathbf{J}_{b_g}^\alpha \delta b_{g_k}\right) + \hat{\alpha}_{b_{k+1}}^{b_k}}{\delta \mathbf{b}_{gk}} = -\mathbf{J}_{b_g}^\alpha
\end{aligned} \tag{83}$$

$$\begin{aligned}
\frac{\partial \delta \theta_{b_{k+1}}^{b_k}}{\partial \mathbf{b}_{gk}} &= \lim_{\delta \mathbf{b}_{gk} \rightarrow 0} \frac{2 \left[\left(\hat{\gamma}_{b_{k+1}}^{b_k} \otimes \left[\frac{1}{2} \mathbf{J}_{b_g}^\gamma \delta \mathbf{b}_{gk} \right] \right)^{-1} \otimes (\mathbf{q}_{b_k}^w)^{-1} \otimes \mathbf{q}_{b_{k+1}}^w \right]_{xyz} - 2 \left[\left(\hat{\gamma}_{b_{k+1}}^{b_k} \right)^{-1} \otimes (\mathbf{q}_{b_k}^w)^{-1} \otimes \mathbf{q}_{b_{k+1}}^w \right]_{xyz}}{\delta \mathbf{b}_{gk}} \\
&= \lim_{\delta \mathbf{b}_{gk} \rightarrow 0} \frac{2R \left[\left(\hat{\gamma}_{b_{k+1}}^{b_k} \right)^{-1} \otimes (\mathbf{q}_{b_k}^w)^{-1} \otimes \mathbf{q}_{b_{k+1}}^w \right] \begin{bmatrix} 0 \\ -\frac{1}{2} \mathbf{J}_{b_g}^\gamma \delta \mathbf{b}_{gk} \end{bmatrix}}{\delta \mathbf{b}_{gk}} \\
&= -R \left[\left(\hat{\gamma}_{b_{k+1}}^{b_k} \right)^{-1} \otimes (\mathbf{q}_{b_k}^w)^{-1} \otimes \mathbf{q}_{b_{k+1}}^w \right]_{3 \times 3} \mathbf{J}_{b_g}^\gamma
\end{aligned} \tag{84}$$

As the same as (83) and (84), we have

$$\begin{aligned}
\frac{\partial \delta \boldsymbol{\beta}_{b_{k+1}}^{b_k}}{\partial \mathbf{v}_{b_k}^w} &= -\mathbf{R}_w^{b_k} \\
\frac{\partial \delta \boldsymbol{\beta}_{b_{k+1}}^{b_k}}{\partial \mathbf{b}_{ak}} &= -\mathbf{J}_{b_a}^\beta
\end{aligned} \tag{85}$$

$$\begin{aligned}
\frac{\partial \delta \boldsymbol{\beta}_{b_{k+1}}^{b_k}}{\partial \mathbf{b}_{gk}} &= -\mathbf{J}_{b_g}^\beta \\
\frac{\partial \delta \mathbf{b}_a}{\partial \mathbf{b}_{ak}} &= -\mathbf{I} \\
\frac{\partial \delta \mathbf{b}_g}{\partial \mathbf{b}_{gk}} &= -\mathbf{I}
\end{aligned} \tag{86}$$

3) $\mathbf{J}[2]$:

$$\begin{aligned} \frac{\partial \delta \alpha_{b_{k+1}}^{b_k}}{\partial \mathbf{p}_{b_{k+1}}^w} &= \lim_{\delta \mathbf{p}_{b_{k+1}}^w \rightarrow 0} \frac{\mathbf{R}_w^{b_k} (\mathbf{p}_{b_{k+1}}^w + \delta \mathbf{p}_{b_{k+1}}^w - \mathbf{p}_{b_k}^w - \mathbf{v}_{b_k}^w \Delta t_k + \frac{1}{2} \mathbf{g}^w \Delta t_k^2) - \hat{\alpha}_{b_{k+1}}^{b_k} - \delta \alpha_{b_{k+1}}^{b_k}}{\delta \mathbf{p}_{b_{k+1}}^w} \\ &= \mathbf{R}_w^{b_k} \end{aligned} \quad (87)$$

$$\begin{aligned} \frac{\partial \delta \boldsymbol{\theta}_{b_{k+1}}^{b_k}}{\partial \mathbf{q}_{b_{k+1}}^w} &= \lim_{\delta \boldsymbol{\theta}_{b_{k+1}}^w \rightarrow 0} \frac{2 \left[\left(\hat{\boldsymbol{\gamma}}_{b_{k+1}}^{b_k} \right)^{-1} \otimes (\mathbf{q}_{b_k}^w)^{-1} \otimes \left[\mathbf{q}_{b_{k+1}}^w \otimes \left[\frac{1}{2} \delta \boldsymbol{\theta}_{b_{k+1}}^w \right] \right] \right]_{xyz} - 2 \left[\left(\hat{\boldsymbol{\gamma}}_{b_{k+1}}^{b_k} \right)^{-1} \otimes (\mathbf{q}_{b_k}^w)^{-1} \otimes \mathbf{q}_{b_{k+1}}^w \right]_{xyz}}{\delta \boldsymbol{\theta}_{b_{k+1}}^w} \\ &= L \left[\left(\hat{\boldsymbol{\gamma}}_{b_{k+1}}^{b_k} \right)^{-1} \otimes (\mathbf{q}_{b_k}^w)^{-1} \otimes \mathbf{q}_{b_{k+1}}^w \right]_{3 \times 3} \end{aligned} \quad (88)$$

4) $\mathbf{J}[3]$:

$$\begin{aligned} \frac{\partial \delta \boldsymbol{\beta}_{b_{k+1}}^{b_k}}{\partial \mathbf{v}_{b_{k+1}}^w} &= \mathbf{R}_w^{b_k} \\ \frac{\partial \delta \mathbf{b}_a}{\partial \mathbf{b}_{ak+1}} &= -\mathbf{I} \\ \frac{\partial \delta \mathbf{b}_g}{\partial \mathbf{b}_{gk+1}} &= -\mathbf{I} \end{aligned} \quad (89)$$

C. Proofs of The Jacobian of The Vision Model

Given (71) and (72), we have

1) $\mathbf{J}[0]$:

$$\begin{aligned} \frac{\partial \tilde{\mathbf{P}}_l^{c_j}}{\partial \mathbf{q}_{b_i}^w} &= \lim_{\delta \boldsymbol{\theta}_{b_i}^{b_i} \rightarrow 0} \frac{\mathbf{R}_b^c \left\{ \mathbf{R}_w^{b_j} \left[\mathbf{R}_{b_i}^w \exp(\delta \boldsymbol{\theta}_{b_i}^{b_i} \times) \left(\mathbf{R}_c^b \frac{1}{\lambda_l} \bar{\mathbf{P}}_l^{c_i} + \mathbf{P}_c^b \right) + \mathbf{P}_{b_i}^w - \mathbf{P}_{b_j}^w \right] - \mathbf{P}_c^b \right\} - \tilde{\mathbf{P}}_l^{c_j}}{\delta \boldsymbol{\theta}_{b_i}^{b_i}} \\ &= \lim_{\delta \boldsymbol{\theta}_{b_i}^{b_i} \rightarrow 0} \frac{\mathbf{R}_b^c \mathbf{R}_w^{b_j} \mathbf{R}_{b_i}^w (\mathbf{I} + \delta \boldsymbol{\theta}_{b_i}^{b_i} \times) \left(\mathbf{R}_c^b \frac{1}{\lambda_l} \bar{\mathbf{P}}_l^{c_i} + \mathbf{P}_c^b \right)}{\delta \boldsymbol{\theta}_{b_i}^{b_i}} \\ &= -\mathbf{R}_b^c \mathbf{R}_w^{b_j} \mathbf{R}_{b_i}^w \left[\left(\frac{1}{\lambda_l} \mathbf{R}_c^b \bar{\mathbf{P}}_l^{c_i} + \mathbf{P}_c^b \right) \times \right] \end{aligned} \quad (90)$$

2) **J**[1]:

$$\begin{aligned}
\frac{\partial \tilde{\mathbf{P}}_l^{c_j}}{\partial \mathbf{q}_{b_j}^w} &= \lim_{\delta \theta_{b_j}^{b_j} \rightarrow 0} \frac{\mathbf{R}_b^c \left\{ \exp(\delta \theta_{b_j}^{b_j} \times) \mathbf{R}_w^{b_j} \left[\mathbf{R}_{b_i}^w \left(\mathbf{R}_c^b \frac{1}{\lambda_l} \bar{\mathbf{P}}_l^{c_i} + \mathbf{P}_c^b \right) + \mathbf{P}_{b_i}^w - \mathbf{P}_{b_j}^w \right] - \mathbf{P}_c^b \right\} - \tilde{\mathbf{P}}_l^{c_j}}{\delta \theta_{b_j}^{b_j}} \\
&= \lim_{\delta \theta_{b_j}^{b_j} \rightarrow 0} \frac{\mathbf{R}_b^c \left\{ \left(\mathbf{I} - \delta \theta_{b_j}^{b_j} \times \right) \mathbf{R}_w^{b_j} \left[\mathbf{R}_{b_i}^w \left(\mathbf{R}_c^b \frac{1}{\lambda_l} \bar{\mathbf{P}}_l^{c_i} + \mathbf{P}_c^b \right) + \mathbf{P}_{b_i}^w - \mathbf{P}_{b_j}^w \right] \right\}}{\delta \theta_{b_j}^{b_j}} \\
&= \mathbf{R}_b^c \left\{ \left[\mathbf{R}_w^{b_j} \left(\mathbf{R}_{b_i}^w \left(\mathbf{R}_c^b \frac{1}{\lambda_l} \bar{\mathbf{P}}_l^{c_i} \right) + \mathbf{P}_{b_i}^w - \mathbf{P}_{b_j}^w \right) \right] \times \right\} \\
&\quad (91)
\end{aligned}$$

3) **J**[2]:

$$\begin{aligned}
\frac{\partial \tilde{\mathbf{P}}_l^{c_j}}{\partial \mathbf{q}_c^b} &= \lim_{\delta \theta_c^{c'} \rightarrow 0} \frac{\exp(\delta \theta_c^{c'}) \mathbf{R}_b^c \left\{ \mathbf{R}_w^{b_j} \left[\mathbf{R}_{b_i}^w \left(\mathbf{R}_c^b \exp(\delta \theta_c^{c'}) \frac{1}{\lambda_l} \bar{\mathbf{P}}_l^{c_i} + \mathbf{P}_c^b \right) + \mathbf{P}_{b_i}^w - \mathbf{P}_{b_j}^w \right] - \mathbf{P}_c^b \right\} - \tilde{\mathbf{P}}_l^{c_j}}{\delta \theta_c^{c'}} \\
&= \lim_{\delta \theta_c^{c'} \rightarrow 0} \frac{\left(\mathbf{I} - \delta \theta_c^{c'} \times \right) \mathbf{R}_b^c \left\{ \mathbf{R}_w^{b_j} \mathbf{R}_{b_i}^w \mathbf{R}_c^b \left(\mathbf{I} + \delta \theta_c^{c'} \times \right) \frac{1}{\lambda_l} \bar{\mathbf{P}}_l^{c_i} + \mathbf{R}_w^{b_j} \mathbf{R}_{b_i}^w \mathbf{P}_c^b + \mathbf{R}_w^{b_j} \left(\mathbf{P}_{b_i}^w - \mathbf{P}_{b_j}^w \right) - \mathbf{P}_c^b \right\}}{\delta \theta_c^{c'}} \\
&\approx \left\{ \mathbf{R}_b^c \left[\mathbf{R}_w^{b_j} \mathbf{R}_{b_i}^w \mathbf{P}_c^b + \mathbf{R}_w^{b_j} \left(\mathbf{P}_{b_i}^w - \mathbf{P}_{b_j}^w \right) - \mathbf{P}_c^b \right] \right\} \times + \\
&\quad \left(\mathbf{R}_b^c \mathbf{R}_w^{b_j} \mathbf{R}_{b_i}^w \mathbf{R}_c^b \frac{1}{\lambda_l} \bar{\mathbf{P}}_l^{c_i} \right) \times - \mathbf{R}_b^c \mathbf{R}_w^{b_j} \mathbf{R}_{b_i}^w \mathbf{R}_c^b \left(\frac{1}{\lambda_l} \bar{\mathbf{P}}_l^{c_i} \times \right) \\
&\quad (92)
\end{aligned}$$

Reference

- [1] T. Qin, P. Li, and S. Shen, "Vins-mono: A robust and versatile monocular visual-inertial state estimator," *IEEE Transactions on Robotics*, vol. 34, pp. 1004-1020, 2018.
- [2] T. Qin, P. Li, and S. Shen. (2017). *VINS-Mono*. Available: <https://github.com/HKUST-Aerial-Robotics/VINS-Mono>
- [3] C. Forster, L. Carlone, F. Dellaert, and D. Scaramuzza, "IMU preintegration on manifold for efficient visual-inertial maximum-a-posteriori estimation," 2015.
- [4] C. Forster, L. Carlone, F. Dellaert, and D. Scaramuzza, "On-Manifold Preintegration for Real-Time Visual-Inertial Odometry," *IEEE Transactions on Robotics*, vol. 33, pp. 1-21, 2016.
- [5] J. Solà. (2017, November 01). Quaternion kinematics for the error-state Kalman filter. *arXiv e-prints*. Available: <https://ui.adsabs.harvard.edu/#abs/2017arXiv171102508S>
- [6] V. Lepetit, F. Moreno-Noguer, and P. Fua, "Epnnp: An accurate o (n) solution to the pnp problem," *International journal of computer vision*, vol. 81, p. 155, 2009.
- [7] W. Ding, D. Xu, X. Liu, D. Zhang, and T. Chen, "Review on Visual Odometry for Mobile Robots," *Acta Automatica Sinica*, vol. 44, pp. 385-400, 2018.
- [8] X. Gao, T. Zhang, Y. Liu, and Q. Yan, *Fourteen lectures of Visual SLAM: From Theory to Practice*. Beijing: Publishing House of Electronics Industry 2017.
- [9] S. Agarwal, K. Mierle, and Others. *Ceres Solver*. Available: <http://ceres-solver.org>
- [10] G. Sibley, L. Matthies, and G. Sukhatme, "Sliding window filter with application to planetary landing," *Journal of Field Robotics*, vol. 27, pp. 587-608, 2010.
- [11] T. Qin, J. Pan, S. Cao, and S. Shen. (2019, January 01). A General Optimization-based Framework for Local Odometry Estimation with Multiple Sensors. *arXiv e-prints*. Available: <https://ui.adsabs.harvard.edu/abs/2019arXiv190103638Q>
- [12] T. Qin, S. Cao, J. Pan, and S. Shen. (2019, January 01). A General Optimization-based Framework for Global Pose Estimation with Multiple Sensors. *arXiv e-prints*. Available: <https://ui.adsabs.harvard.edu/abs/2019arXiv190103642Q>
- [13] E. H. Shin, "Estimation techniques for low-cost inertial navigation," PhD, Department of Geomatics Engineering, The University of Calgary Calgary, Canada, 2005.